CHARACTERISTICS OF DIFFERENT MATERIALS ON HIGH-GRADIENT EXPERIMENTS

K. Yokoyama#, T. Higo, S. Fukuda, S. Matsumoto, Y. Higashi, N. Kudoh, Y. Watanabe,
KEK, Ibaraki, Japan

Abstract

RF breakdown is one of the major problems encountered in the development of accelerating structures that operate at high fields since the acceleration field is limited by the damage caused to metal surfaces. We examine electrical discharge characteristics such as breakdown rates and conduct surface observations of various materials in order to investigate the possibility of the stable operation of accelerating structures for high-field accelerations; a similar fundamental research has also been conducted at CERN and SLAC [1, 2,]. High-gradient RF breakdown studies have been in progress at Nextef (New X-band Test Facility at KEK) since 2006 [3, 4, 5]. In order to investigate the characteristics of various materials at high-gradient RF breakdown, we have performed high-gradient experiments by using narrow waveguides having a field of around 200 MV/m at a power of 100 MW. Copper (OFC) and stainless-steel (AISI-316L) waveguides were tested in order to perform high-gradient experiments at Nextef. The result of the experiment conducted at XTF (Old X-band Test Facility at KEK) suggested that the stainless-steel waveguide had a better performance than the copper waveguide, and it exhibited a lesser number of RF breakdowns at a higher electric field. This paper reports the results of breakdown rates and observations of the surface of stainless-steel waveguide subjected to high-gradient experiments.

HIGH-GRADIENT EXPERIENTS

Narrow Waveguide

A narrow waveguide was designed to obtain a group velocity of around 0.3 c, which is used to drive an LC accelerating structure, and a field gradient of approximately 200 MV/m at an RF power of 100 MW at the centre, as shown in Fig. 1. The geometry was transformed from the X-band rectangular waveguide (WR90). The height and the width were reduced from 10.16 mm to 1 mm and from 22.86 mm (λ_g ~ 32.15 mm) to 14 mm (λ_g ~ 76.59 mm), respectively. A narrow waveguide was constructed from four parts in the manufacture. After annealing in a hydrogen furnace, the narrow waveguide was processed by milling. The parts were chemically polished in an acid solution by 10 μm, following which they were brazed in a hydrogen furnace. A narrow waveguide having a voltage standing wave ratio (VSWR) of less than 1.1 is required for our experiments.

#kazue.yokoyama@kek.jp

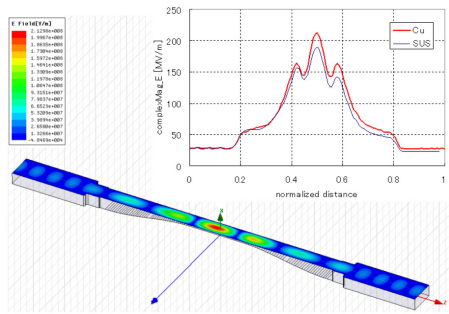

Figure 1: Electric field in a narrow waveguide at an input power of 100 MW obtained by the HFSS calculation.

Experimental Setup

The setup for the high-gradient experiment is shown in Fig. 2. RF power is supplied to the narrow waveguide from a PPM-focused klystron that is operated at 11.424 GHz with a pulse width of 400 ns, pulse repetition rate of 50 Hz, and peak output power of approximately 50 MW. Transmitted and reflected RF waveforms are observed for breakdown events. An RF pulse is detected by using a crystal diode and a digital oscilloscope is used to calculate the power, VSWR, and power loss. All RF pulses are measured, and the digital data for 10 successive pulses is saved in order to analyze the RF waveforms when some interlock controls such as HV, Trig, and RF are tripped. In order to distinguish a breakdown in the narrow waveguide from one that occurs at another location, photomultipliers (PMTs) and acoustic sensors are placed along the waveguide.

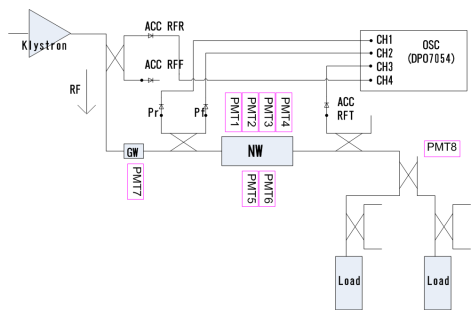

Figure 2: Setup of a high-gradient experiment conducted at Nextef.

During waveguide processing, the RF pulse width is increased from 50 ns to 400 ns, and an RF power of up to 50 MW at a repetition rate of 50 pps is supplied. The increase in the output power and the duration of incremented power are controlled by a computer in accordance with the past processing history depending on the experienced power and the pressure. When the pressure in the waveguide increases, the processing power

is maintained constant until the pressure reaches a normal level. However, in case where the pressure increases significantly, the processing power is decreased, and processing is repeated from a lower power level in order to avoid serious breakdown damages to the waveguide.

RESULTS

RF Processing

The processing history and accumulated data for breakdown events that occur during the processing of #CU002 (copper) and #SUS003 (stainless-steel) waveguides are shown in Figs. 3(a) and (b), respectively. The first high-gradient experiment was conducted over a period of one month at the XTF using the #CU002 waveguide. The RF processing time was restricted to approximately 250 h due to a fixed XTF schedule. Therefore, we could not confirm whether the numbers of break down events were saturated or not but we could not keep operating of #CU002 due to a lot of breakdown. The second high-gradient experiment was conducted at Nextef using the #SUS003 waveguide. The existing interlock controls for RF processing and breakdown measurement systems were replaced with improved interlock controls during the processing of the #SUS003 waveguide. Almost half a year was required to complete the RF processing of RF components such as guard windows, directional couplers, and dummy loads. The RF processing time of the #SUS003 waveguide reached up to approximately 1200 h.

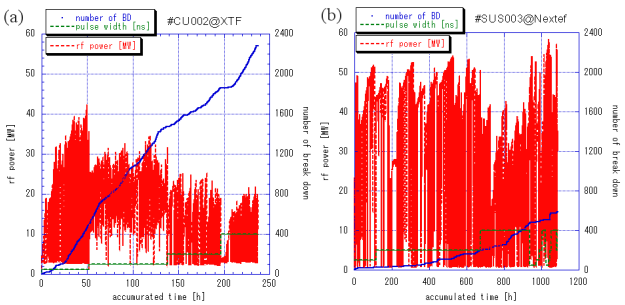

Figure 3: Power history of (a) #CU002 and (b) #SUS003 waveguides during processing.

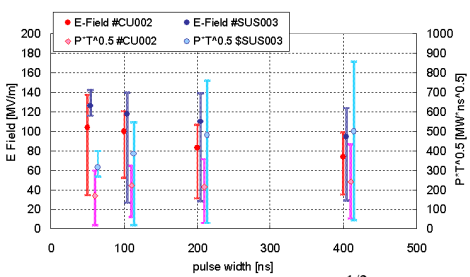

Figure 4: Experienced E-field and $P*T^{1/2}$ for #CU002 and #SUS003 waveguides.

Figure 4 shows the electric field and the temperature-related parameter $P*T^{1/2}$ (the product of the RF power and the square root of the pulse width) as the function of the pulse width of #CU002 and #SUS003. The results of these experiments indicated that the #SUS003 waveguide had a better performance than the #CU002 waveguide in that it exhibited a lesser number of RF breakdowns at a higher electric field. Figure 4 indicates that a higher RF power might be required in order to perform RF processing and to determine the power limit for sustaining a high electric field.

Breakdown Rates

After RF processing, breakdown rates (BDRs) of the waveguide were measured as a function of the RF power and the pulse width in order to investigate their dependence on the material characteristics. A constant power was supplied for approximately 24 h, and the number of breakdown events was recorded. Figure 5 shows the BDRs of the #SUS003 waveguide as a function of the RF power. BDRs for a pulse width less than 100 ns are very low. Although the number of breakdown events fluctuates, it is observed that the BDR increases with power, and the relationship between the BDR and the input power is exponential, as shown in Fig. 5.

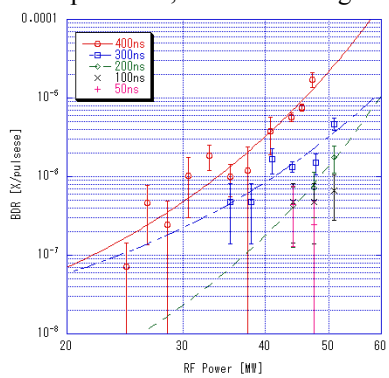

Figure 5: Breakdown rate as a function of pulse width of #SUS003 waveguide.

Surface Observations

The material surfaces were observed using a laser microscope and a SEM. Figure 6 shows a drawing of the waiveguide and a overall picture of #CU002 and #SUS003 after cutting structures for surface observation after high-gradient experiments. Many breakdown (BD) damages were observed in areas that produced a high field on the E-plane surface. Figures 7 (a) and (b) show the laser microscope view and (c) shows the concavoconvex-view of #CU002 by laser scanning around the area. Similarly, Figs. 8 (a), (b), and (c) show the corresponding images of the #SUS003 waveguide. The magnification factor for both figures is the same; (a) 200, (b) 1000, and (c) 1000. Many peaks and valleys (~ 30 μm in height) are detected on the material surface in a high-field region, although details of the peaks observed using the laser microscope are different for the #CU002 and #SUS003 waveguides. In the wider hight region, we observed traces of a single BD and several single-BD patterns. The narrower-height region suffered extensive breakdown damage as a result of which it melted. We believe that #SUS003 melts more than #CU002; however, their peak heights are similar, althogh the fine structure of

these surfaces differ significantly, as shown in Figs. 7(c) and 8(c). Examples of breakdown spots observed on the surfaces of (a) #CU002 and (b) #SUS003 by SEM are shown in Fig. 9. Under an SEM magnification factor of 1000, the breakdown spots in both materials are observed to have a similar melting pattern. Since the surface finishing and processing process of #CU002 differ from those of #SUS003, a precise comparison between the two remains difficult. In the future, we plan to conduct experiments using copper (#CU004) having the same machine-finished surfaces as stainless-steel (#SUS003) in order to obtain a more accurate comparison.

SUMMARY

An experimental setup for conducting RF breakdown studies has almost been established at Nextef in KEK. Breakdown diagnoses including waveform analysis are being developed, and these will be useful for obtaining more reliable measurements of materials. Breakdown tests on different materials are also being performed. The prototypes #CU002 and #SUS003 have been tested under different systems, and their material surfaces have been observed after testing. Initial test results indicate that stainless-steel (#SUS003) probably has higher breakdown durability than copper (#CU002). In the future, we plan to test a narrow waveguide composed of #CU004 using the same system parameters and fabrication method as #SUS003 to validate the results obtained in the case of #CU002.

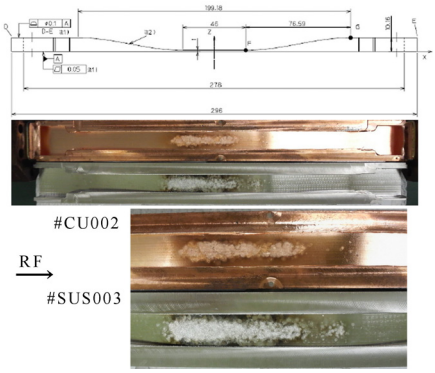

Figure 6: Waveguide drawing and surface #CU002 and #SUS003 after processing.

REFERENCES

[1] A. Descoudre, et. al., "DC Breakdown Experiments for CLIC", Proc. of EPAC08, Genoa, Italy, June 23-27, 2008, pp.577-579.

[2] V. A. Dolgashev, S. G. Tantawi, "RF Breakdown in X-band. Waveguides," TUPLE098, EPAC'02, 3-7 June, 2002, Paris,. France, pp. 2139-2141.

[3] S. Matsumoto, et al., "The Status of Nextef; The X-band Test Facility in KEK", Proc. of LINAC08, Victoria, British Columbia, Canada.

[4] K.Yokoyama, et al., "High Field Performance in Reduced Cross-Sectional X-band Waveguides made of Different Materials", Proc. of PAC07, Albuquerque, NM, USA, pp.2119-2121.

[5] K. Yokoyama, et. al., "High-Gradient Experiments with Narrow Waveguides", Proc. of EPAC08, Genoa, Italy, June 23-27, 2008, pp.2758-2760.

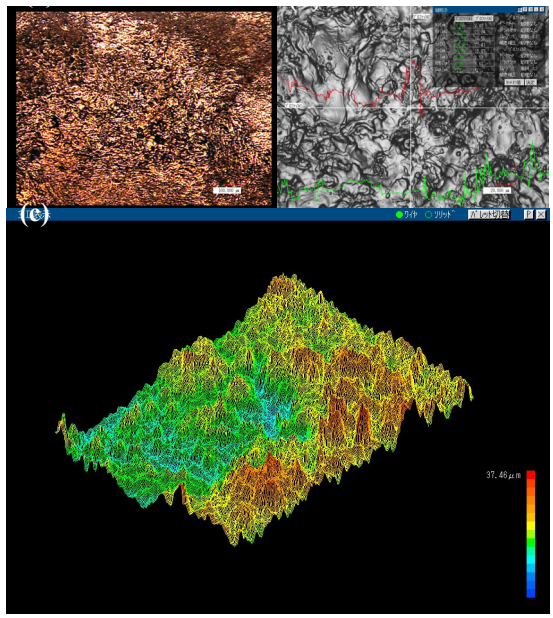

Figure 7: Surface observation of #CU002 by laser microscope. (a) and (b) show examples of the breakdown area at different scales, and (c) provides the birds eye view of laser scanned (b).

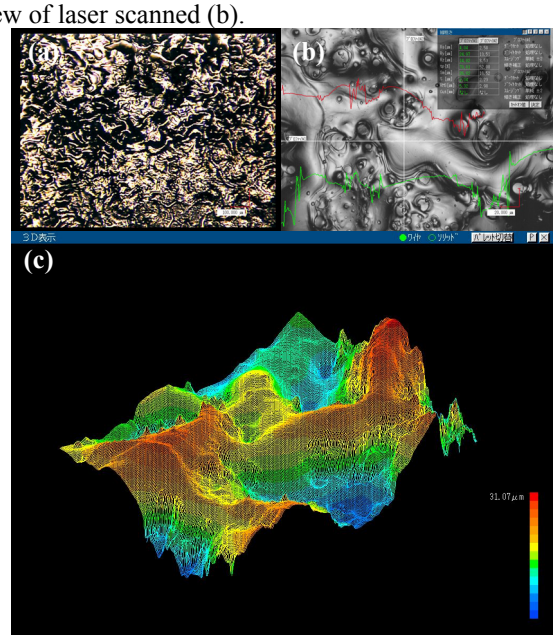

Figure 8: The same as Figure 7 for #SUS003.

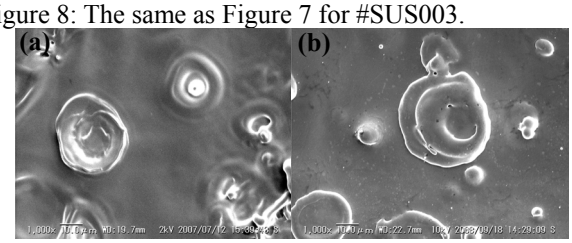

Figure 9: Examples of breakdown spots observed on the surfaces observation of (a) #CU002 and (b) #SUS003 by SEM.